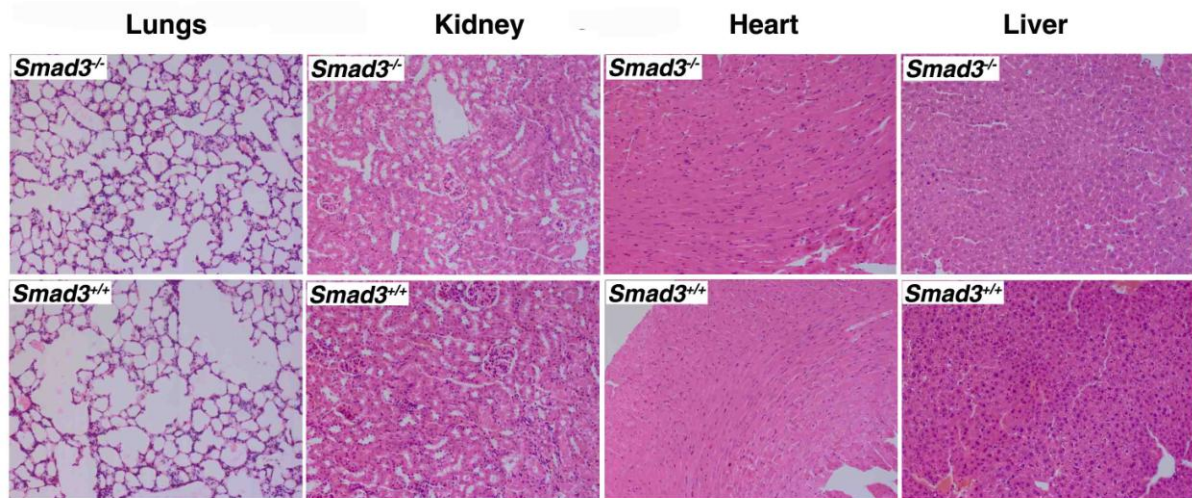


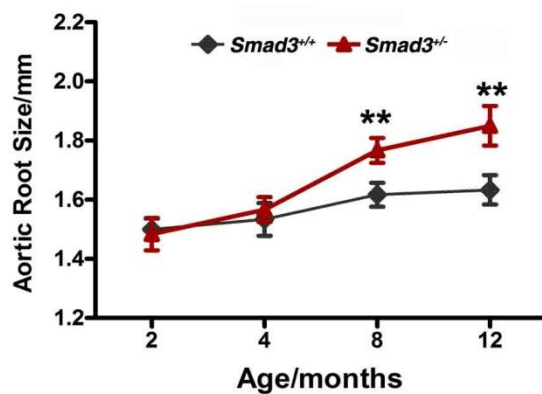
Supplemental Material

Supplemental Figure 1



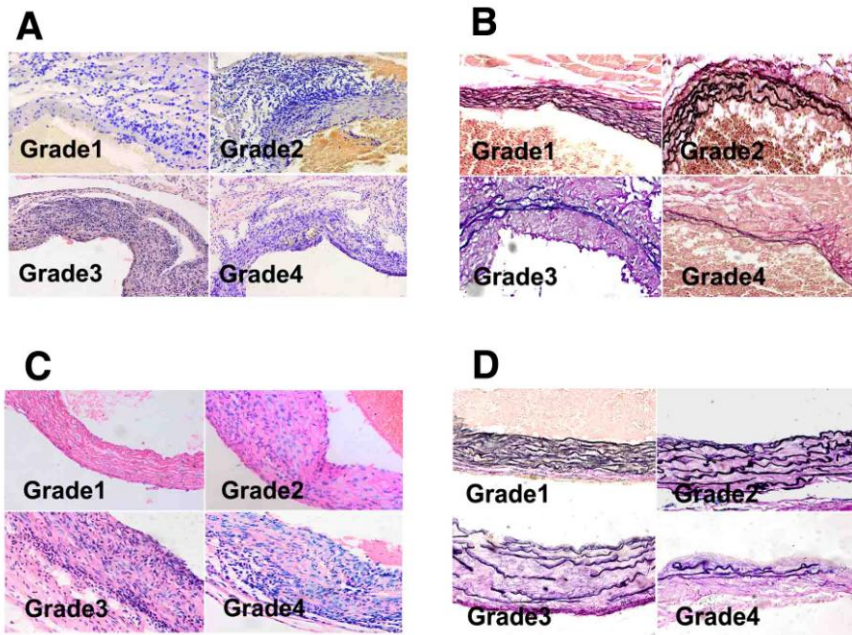
Supplemental Figure 1. Representative HE staining of the lungs, kidney, heart and liver from 1-mo-old *Smad3^{+/+}* and *Smad3^{-/-}* which were showed normal. There are no inflammation was found in these organs. Original magnification, 200 \times .

Supplemental Figure 2



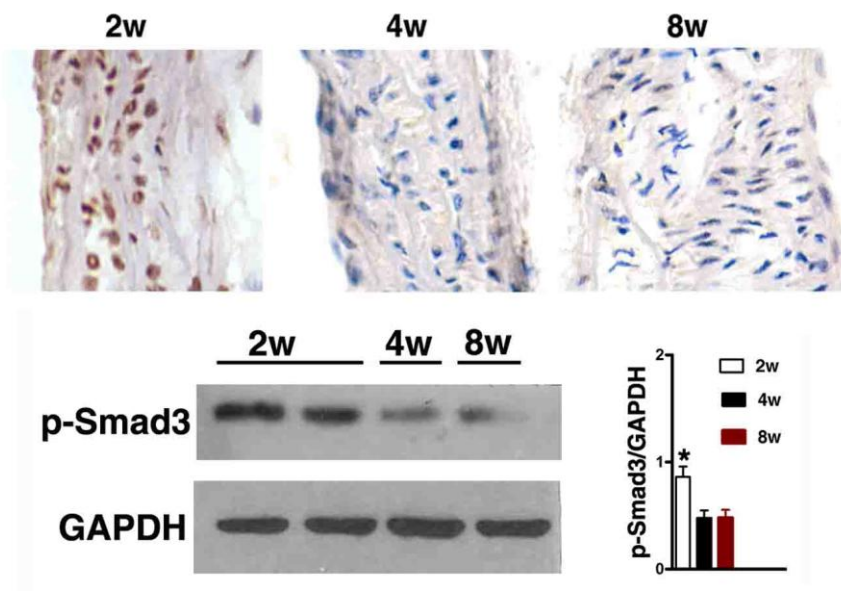
Supplemental Figure 2. Aortic root diameter, measured by echocardiography, at different ages of WT (*Smad3^{+/+}*) (n=6/time points) and *Smad3^{-/-}* (n=7/time points) mice. ** $P < 0.001$ *Smad3^{-/-}* versus WT at the same age.

Supplemental Figure 3



Supplemental Figure 3. Elastin degradation–grading (4 grades) keys (B, D) and inflammatory cell infiltration–grading (4 grades) (A, C) of aortic root (A, B) and ascending aortas (C, D) were shown. Original magnification, 400×.

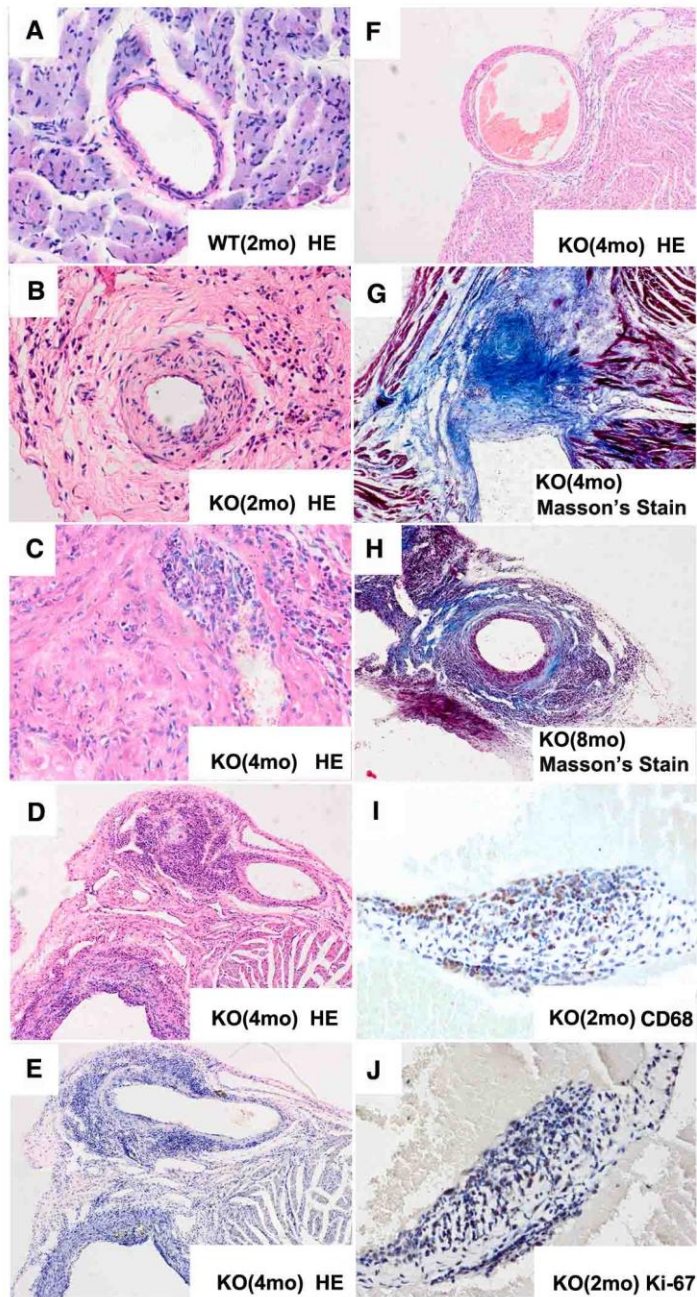
Supplemental Figure 4



Supplemental Figure 4. The expression of p-Smad3 in the *Smad3^{+/+}* mice. The image showed Immunostaining for p-Smad3 on slides of aortic root from *Smad3^{+/+}* aged at 2, 4 and 8 weeks. Representative Western blot showing p-Smad3 levels in

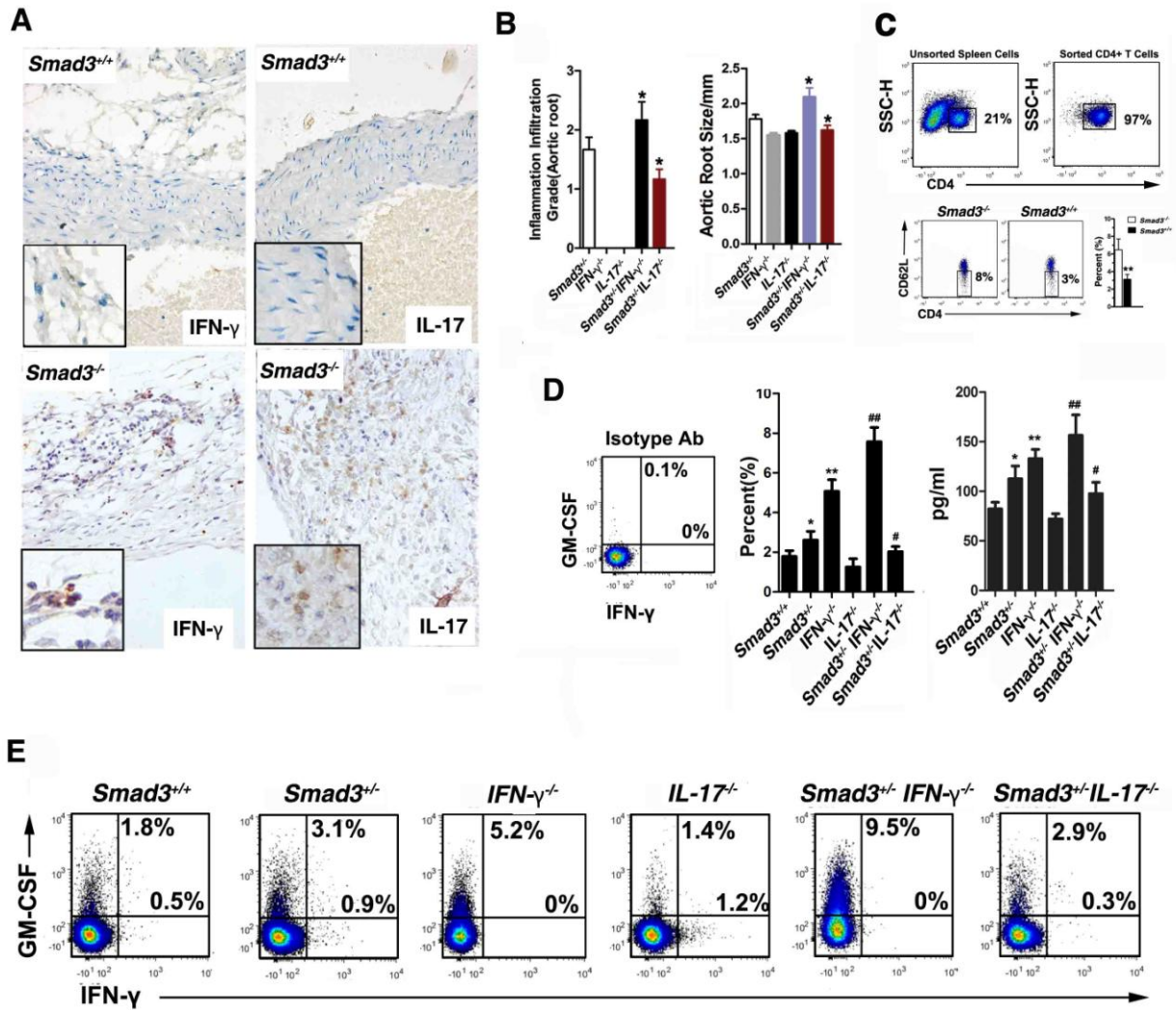
proximal ascending aortas from *Smad3*^{+/+} mice aged at 2, 4 and 8 weeks. The ratio between p-Smad3 to GAPDH levels is shown. **P* < 0.01, vs 4 or 8 weeks. Original magnification, 400×.

Supplemental Figure 5



Supplemental Figure 5. Inflammation in the coronary arteries and aortic valves from *Smad3*^{-/-} mice. **A**, HE staining showing normal coronary arteries from *Smad3*^{+/+} mice. **B**, Intimal thickening. **C**, Inflammatory cells accumulating in the vascular space. **D**, Complete occlusion of the coronary artery. **E, F**, Coronary artery ectasia. **G, H**, Varying degrees of vascular fibrosis. **I, J**, Adhesion of CD68⁺ cells to the aortic valve and expression of Ki-67, a cell proliferation marker. Original magnification, (D, E, F, H):100×; (A,B,C,G): 400×.

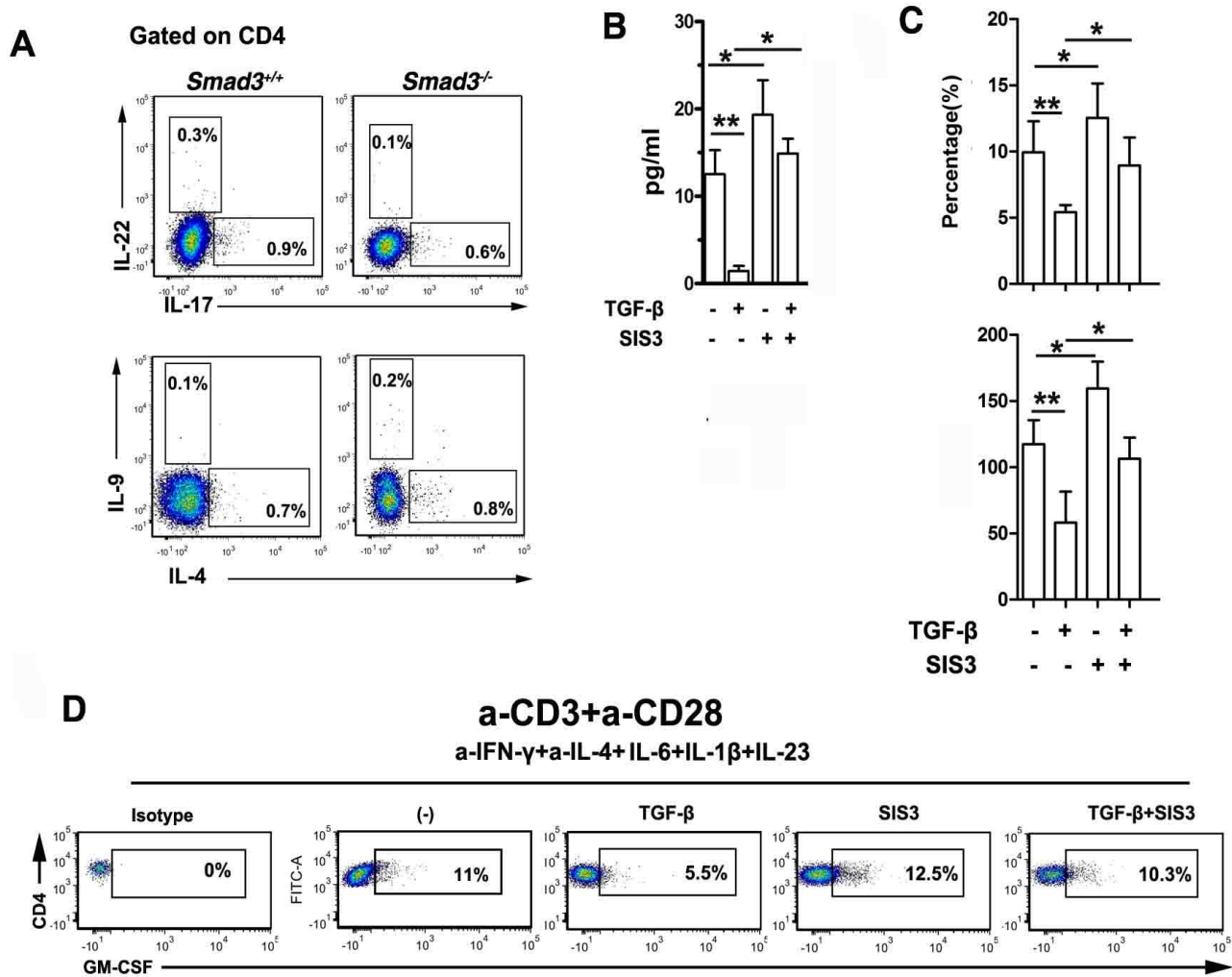
Supplemental Figure 6



Supplemental Figure 6. IFN- γ and IL-17 play opposite role on regulation of GM-CSF secretion by CD4⁺ T cells, which impact the aortic pathological changes of *Smad3*^{-/-} mice. **A**, Immunostaining with the IFN- γ and IL-17 antibody revealed an accumulation of IFN- γ - and IL-17-producing cells in the aortas of *Smad3*^{-/-} mice, and no obvious positive staining was observed in the aortas of *Smad3*^{+/+} mice. Original magnification, 400 \times ; Magnified panels, 1000 \times . **B**, The histograms show different inflammation severity and aortic root size in the aortic roots from 6 genetically engineered mice, which exhibited worse inflammation severity in *Smad3*^{+/-} *IFN- γ* ^{-/-} mice, while *Smad3*^{+/-} *IL-17*^{-/-} mice showed slightly better than the *Smad3*^{+/-} mice. **P* < 0.01 vs *Smad3*^{+/-} mice. **C**, Flow cytometry analysis of the sorting efficiency of CD4⁺ T cells. *Smad3*^{-/-} mice contains more CD4⁺CD62L⁺ cells in the spleen than *Smad3*^{+/+} mice, which showed an activated phenotype. **D**, IFN- γ deficiency promoted GM-CSF secretion in CD4⁺ T cells from WT and *Smad3*^{+/-} mice, while IL-17 deficiency had a slight

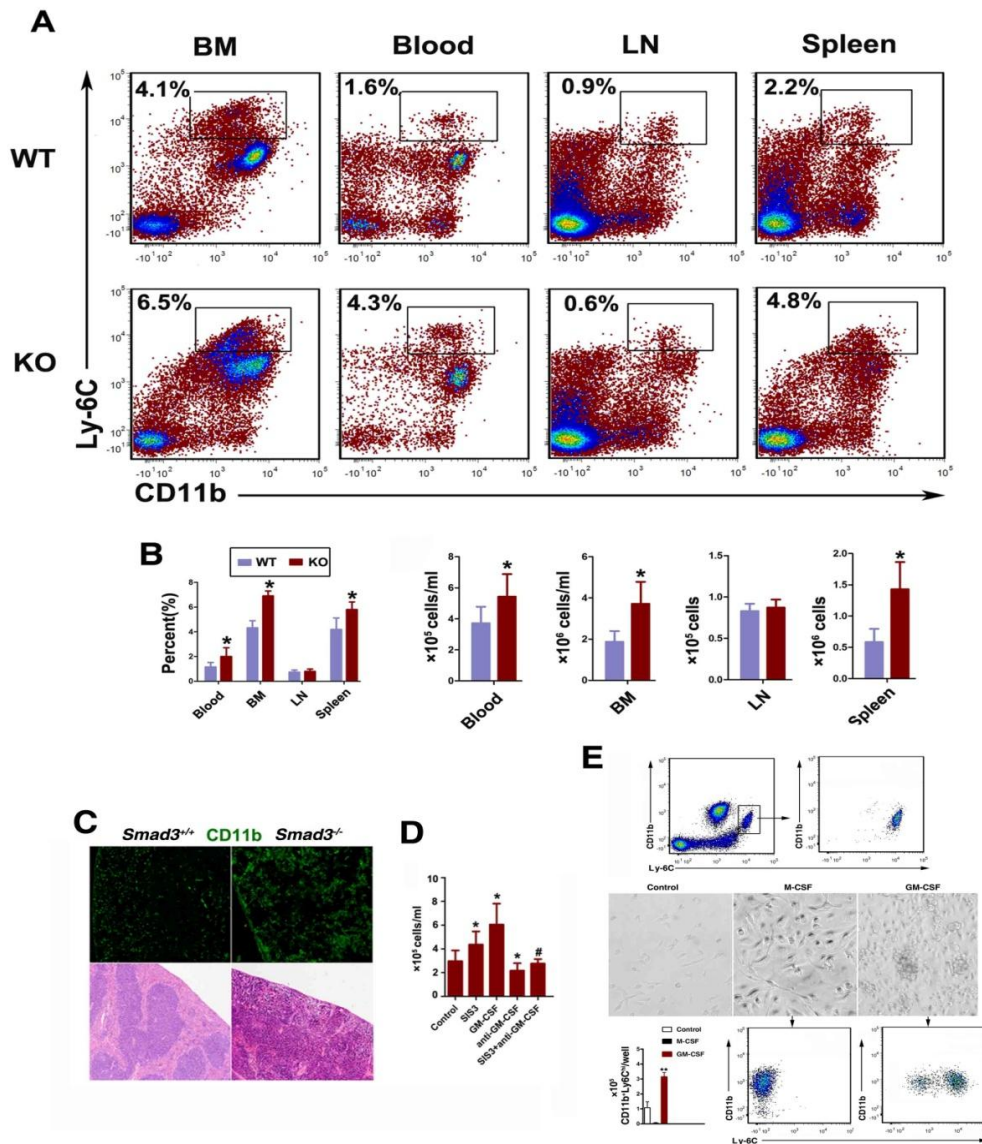
inhibitory effect. The amount of GM-CSF in the supernatants was measured using a specific ELISA kit and was consistent with flow cytometry results. * $P < 0.05$, ** $P < 0.01$ versus WT. # $P < 0.05$, ## $P < 0.01$ versus *Smad3*^{+/-}. **E**, Flow cytometry analysis of the secretion of GM-CSF and IFN- γ by CD4⁺ T cells. Isotype control Abs were added for gating.

Supplemental Figure 7



Supplemental Figure 7. A, Under neutral priming conditions in spleen cells, *Smad3*^{-/-}CD4⁺ T cells appeared to have the same ability to secrete IL-4, IL-9, IL-22, and IL-17. Representative flow cytometry image were shown. **B**, GM-CSF concentration in the suspension were compared when isolated spleen CD4⁺T cells were under neutral priming conditions with or without the addition of TGF- β /SIS3. * $P < 0.05$, ** $P < 0.01$. **C**. Isolated spleen CD4⁺T cells were transformed under GM-CSF priming conditions with or without the addition of TGF- β /SIS3. The percentage of CD4⁺ T cells producing GM-CSF and GM-CSF concentration in the suspension were compared between different groups. * $P < 0.05$, ** $P < 0.01$. **D**. Intracellular cytokine staining was performed to determine the percentage of CD4⁺ T cells producing GM-CSF. Representative flow cytometry image were shown.

Supplemental Figure 8



Supplemental Figure 8. Smad3 inhibition induced GM-CSF-dependent bone marrow and extramedullary hematopoiesis, which induced a relatively high number of CD11b⁺Ly-6C^{hi} cells. **A**, Representative flow cytometry image of blood, spleen, LN and BM cells gated on Ly-6C and CD11b. **B**, *Smad3*^{-/-} mice contained more CD11b⁺Ly-6C^{hi} inflammatory monocytes in the blood, BM and spleen. **P* < 0.05. **C**, Representative HE staining of spleen cells and CD11b immunofluorescence staining showed altered structure of spleen cells and a relatively increased number of CD11b⁺ cells in *Smad3*^{-/-} mice than that in *Smad3*^{+/+} mice. Original magnification, 200 \times . **D**, The percentage and number of CD11b⁺Ly-6C^{hi} in 1ml blood from WT mice received different agents were compared. **P* < 0.05 versus control. #*P* < 0.05 versus SIS3. **E**, Isolated the inflammatory monocytes from the blood of WT mice by flow cytometry, and cultured them with or without GM-CSF or M-CSF. M-CSF could effectively induce the maturation of inflammatory monocytes and their transformation into fusiform wall-adherent cells and they no longer express Ly-6C. GM-CSF maintained the most traits of the cells and promoted their proliferation. Without addition of any cytokines, the inflammatory monocytes hardly proliferated. ***P* < 0.01 versus control. Original magnification, 400 \times .

Supplemental Table 1. Clinical information of study participants

	Case1	Case2
Age(years)	35	40
Gender	F	M
Smoking	NO	NO
Hypertension	NO	NO
Atrial fibrillation	YES	NO
Thoracic aortic aneurysm	YES	YES
Diameter of aneurysm(cm)	6.4	5.4
Abdominal aortic aneurysm	NO	NO
Aortic dissection/rupture	NO	NO
Aortic tortuosity	YES	NO
Ventricular hypertrophy	NO	YES
Mitral valve anomalies	YES	NO
Congenital heart malformation	NO	NO
Osteoarthritis of \geq 1 joint	YES	YES
Joint laxity	NO	NO
Painful joints	YES	YES
Skeletal anomalies	NO	YES
Hypertelorism	NO	YES
Abnormal palate or uvula	NO	NO
Velvety skin	NO	NO